

The petrosal ganglion of the adult cat: neuronal count, sectional area, and their respective distributions

J ALCAYAGA, J ARROYO, MI FONT and OC GUTIERREZ

Laboratorio de Neurobiología, Departamento de Biología,
Facultad de Ciencias, Universidad de Chile, Santiago, Chile

The petrosal ganglion contains most of the perikarya of sensory neurons of the glossopharyngeal nerve. We studied the number and size of neuronal somata in 4 petrosal ganglia from adult cats. Ganglia were serially sectioned in length at 8 μm , sections drawn through a projection microscope, and those neuronal profiles presenting nuclei and nucleoli on each section were counted and their areas measured.

The number of neurons ranged from 2311 to 3429 (2908 ± 271 ; mean \pm SEM). Neurons were symmetrically distributed around the longitudinal axes of most ganglia, with a skewed distribution in only one ganglion. The sectional area of most neurons (> 98%) ranged between 250 and 1725 μm^2 , with median values of 667-963 μm^2 . Area distributions were significantly different, but differences never exceeded 8.2% in related area bins. The ganglion presenting a skewed count distribution and the highest median area departed from the rest, with differences surpassing 25%. We conclude that the neuronal population of the petrosal ganglion of the cat is regular both with respect to the number and the size of its constituents, with departures from this pattern probably reflecting individual variations.

Key terms: neuronal somata area, neuronal somata distribution, neuronal somata number, petrosal ganglion, profile size distribution.

INTRODUCTION

The petrosal ganglion is the larger of the two sensory ganglia of the glossopharyngeal (IXth) nerve. Its neurons provide sensory innervation to the pharynx and tympanic cavity, to taste and tactile receptors of the posterior third of the tongue, and to chemoreceptors and baroreceptors of the carotid body and sinus, respectively. However, there is limited information on the neuronal constituents of the petrosal ganglion. This consists only of an abstract related to an estimate of the number of neurons in one ganglion (Foley and Sackett, 1950) and a mention to the distribution of neuronal perikarya along the glossopharyngeal nerve

(data of Zapata reported within a review by Eyzaguirre and Zapata, 1984). Other studies are only concerned with the localization and size of subsets of the petrosal neurons innervating particular territories (Berger, 1980; Claps and Torrealba, 1988; Claps *et al.*, 1989; De Groat *et al.*, 1979; Kalia and Davies, 1978; Katz and Black, 1986; Nomura and Mizuno, 1982; Torrealba, 1992; Torrealba and Claps, 1988).

There are few studies on the electrophysiological characteristics of petrosal ganglion neurons (Morales *et al.*, 1987), particularly those innervating the carotid body and sinus (Belmonte and Gallego, 1983; Gallego, 1983). Furthermore, experiments have been carried out to characterize

the activity of petrosal ganglion neurons following disconnection, reinnervation or cross-reinnervation of their peripheral targets, particularly taste buds and carotid chemoreceptors (see Eyzaguirre *et al.*, 1983). More recently, co-cultures of visceral sensory ganglion neurons and chemoreceptor cells have been performed (Alcayaga, 1995; Alcayaga and Eyzaguirre, 1990; Goldman *et al.*, 1987). However, the interpretation and design of additional physiological experiments requires comprehensive data on the morphology of petrosal ganglion neurons, since morphological data available from dorsal root and nodose ganglia cannot be freely extrapolated to the petrosal ganglion. Thus, we studied the number, size and distribution of neuronal perikarya in petrosal ganglia of adult cats, to provide detailed information on their entire neuronal population.

METHODS

Four adult cats (two males and two females) weighing from 2.0 to 3.6 kg, were anaesthetized with sodium pentobarbitone (40 mg/kg, ip). The glossopharyngeal nerve was identified at the level of the carotid bifurcation through an incision in the ventral midline of the neck, and it was followed into the jugular foramen of the cranium. The bulla tympanica and ventral wall of the jugular foramen were gently eroded to expose the petrosal ganglion, which was then separated from surrounding tissues, and its central and peripheral processes were cut, leaving about 2 mm nerve stumps on each side of the ganglion. Cats were sacrificed with an overdose of the anaesthetic.

The right petrosal ganglion from a female cat and three left petrosal ganglia from remaining cats were immediately placed in a topographic fixative (g/100 ml: HgCl₂, 4.5; NaCl, 0.5; trichloroacetic acid, 2.0; acetic acid, 4.18; formaldehyde, 6.0) for 24 h, dehydrated, embedded in paraffin (52°C, 24 h), aligned, trimmed and sectioned longitudinally every 8 µm. Sections were serially mounted on gelatinized slides, deparaffinized and stained with Heidenhain's azocarmine-aniline method (Gabe, 1968).

Each section of the ganglion was visualized through a projection microscope to a

final enlarging of 440X, and every neuronal profile presenting nucleus and nucleolus was drawn. To avoid multiple measures of the same neuron, because of eventual splitting or presence of double nucleoli, each drawn section was projected onto the preceding and subsequent sections; then whenever a double count was found, the neuronal profile with the smaller nucleolus was deleted from the drawing. On each section, neurons showing their nuclei and whole nucleoli were counted and their areas measured from the contours, through a digitizing tablet and commercial software (Sigma Scan, Jandel Scientific).

Statistical analyses of neuronal numbers and area distributions were performed through Kolmogorov-Smirnoff tests. Differences between the neuronal counts and areas were evaluated through Kruskal-Wallis rank tests with multiple comparisons (Theodorsson-Norheim, 1986).

RESULTS

In longitudinal sections, the petrosal ganglion appears as an ellipsoidal enlargement of the glossopharyngeal nerve. Neuronal profiles were scanty in the most superficial sections, but increased towards those including the innermost longitudinal axis of each ganglion (Fig 1). Neurons were distributed in conspicuous groups, containing variable numbers of cells, separated by bundles of fibers, thus giving the appearance of islands. However, when analyzed throughout the depth of the ganglion, most of these neuronal assemblies coalesced, forming a cellular continuum. Nerve fibers were uncommon near the perimeter of the ganglion, but were not confined to a particular location in the section.

The number of tissue-containing sections obtained from each ganglion were 76, 124, 131 and 116, with perikarya present only in 54, 63, 63 and 75 sections, respectively. Thus, neurons were confined to about 50-70% of the total ganglion width, with nerve fibers representing most of the tissue in remaining sections. The total number of neuronal somata counted in the petrosal ganglia were 2311, 3429, 3298 and 2594 (2908 ± 271 ; mean \pm SEM; coefficient of

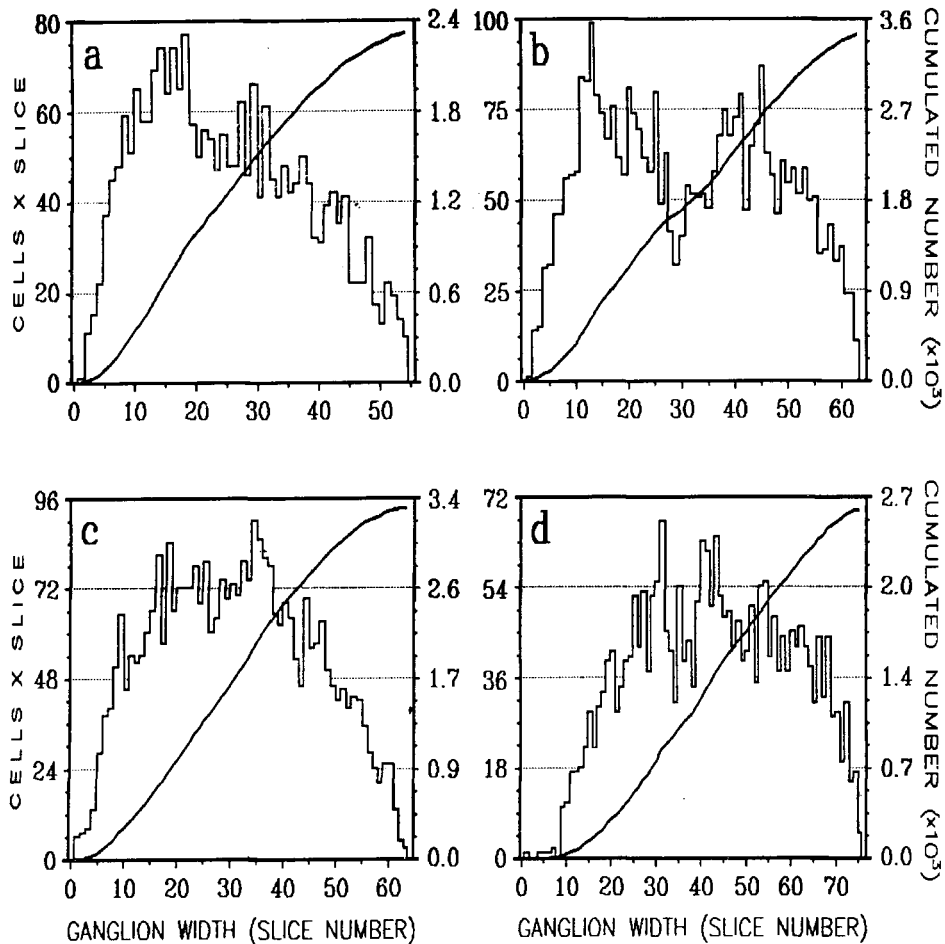


Fig 1. Cell counts per slice (histograms and left ordinates) and cumulated cell counts (ascending lines and right ordinates) of four petrosal ganglia. Left ganglia from male cats (a, b) and female cat (d); right ganglion from female cat (c).

variation 0.19), for the two male and the two female cats, respectively, presenting no sex related differences ($p > 0.9$). The number of neurons showing both nucleus and nucleolus first increased with the slice serial number, reached a peak, and then decreased towards the other surface (Fig 1). The neuronal count distribution of the ganglia from female cats appeared to have a wide plateau, comprising about two thirds of the ganglion thickness (Fig 1c, d). Conversely, the ganglia from male cats seemed to have an asymmetric perikaryal distribution, which appeared more concentrated toward one surface of the ganglia (Fig. 1a, b). The statistical analysis shows significant ($p < 0.05$; Kolmogorov-Smirnoff test) differences in perikarya distributions among the petrosal ganglia, although

none exceeds 8.2% when the widths of the ganglia are expressed in percentages.

Despite the already mentioned differences, the cumulative distribution of perikarya (Fig 1; thick lines) within each ganglion showed that about 50% of the neuronal somata were allocated in about one half of the width of the cellular portion of the ganglion. As the different ganglia were sectioned at no preferential longitudinal plane, standardized cumulative distributions were constructed, either following increasing slice serial number (direct) or decreasing serial number (reverse) direction, and then both were compared (Fig 2; open circles). These scatter diagrams indicate that the distributions are different, diverging from the identity line, specially towards the innermost portions. In

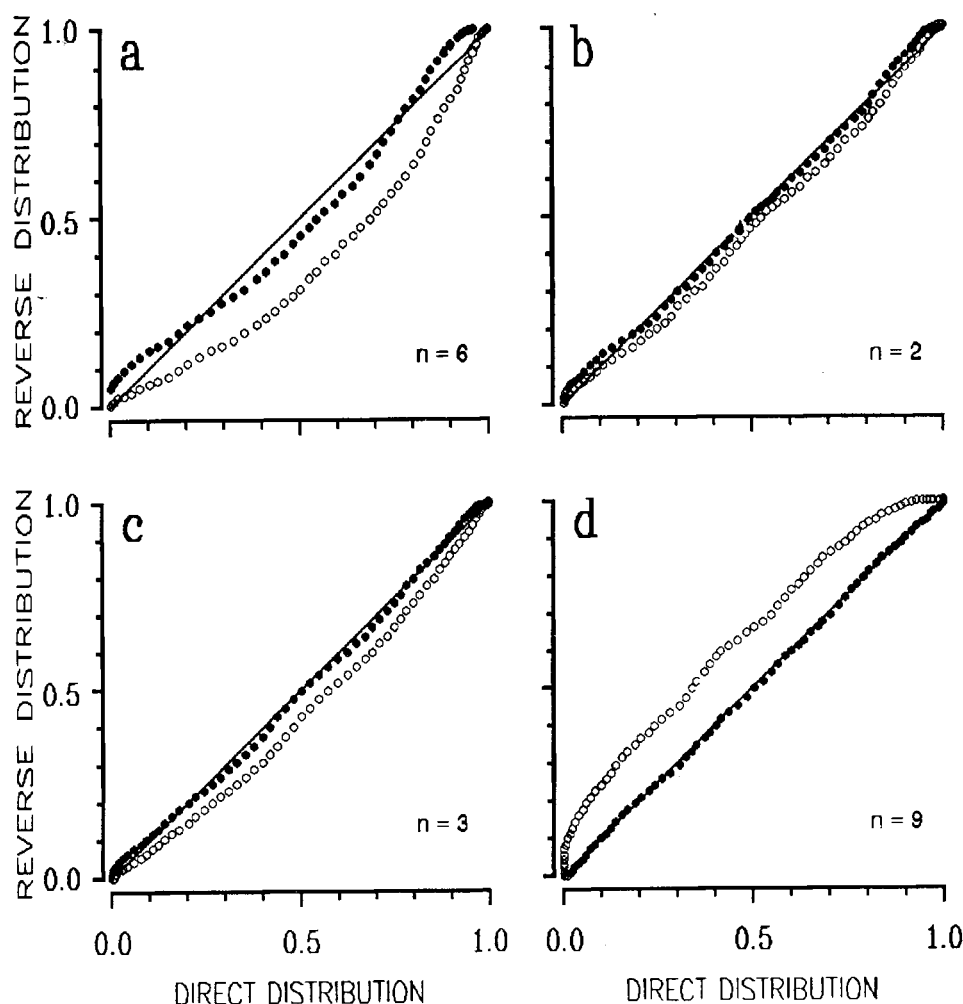


Fig 2. Scatter diagrams of reverse (ordinates) against direct (abscissae) cumulated distributions of perikarya across petrosal ganglia in 4 cats. **a, b, c** and **d** as in Figure 1. Scatter plots before (○) and after (●) displacing one distribution against the other by *n* points. Direct distribution displaced by 6 points (a), 2 points (b) and 3 points (c) to the right or by 9 points (d) to the left. Solid lines represent identity lines.

all four cases, direct and reverse standardized distributions were significantly different ($p < 0.01$; Kolmogorov-Smirnoff test). However, the distributions can be made to nearly overlap and the standardized scatter diagram to approach the identity line, if the distributions are slightly displaced one towards the other between 3 and 12% of their total widths (Fig 2; filled circles), until the square difference sum attained a minimum. This displacement reduced count distribution differences below the statistical significance level ($p > 0.05$; Kolmogorov-Smirnoff test) in three of the four ganglia (Fig 2b-d), the difference being retained in one ganglion from a male cat (Fig 2a). This displacement

effect indicates that most of the observed differences were indeed generated by the extremes of the distributions, with the core portions of the ganglia presenting axial symmetries.

Measurement of neuronal somata profile areas of the four petrosal ganglia shows that most perikarya (>98%) ranged between $225 \mu\text{m}^2$ and $1725 \mu\text{m}^2$, with neurons below $225 \mu\text{m}^2$ contributing less than 0.14% to the total population (Fig 3). Analysis of the perikaryal areas of the four petrosal ganglia showed significant differences (Kruskal-Wallis test; $p < 0.001$) within them, but two ganglia had no statistical differences between their perikaryal areas ($p > 0.05$; Fig 3b, d). The

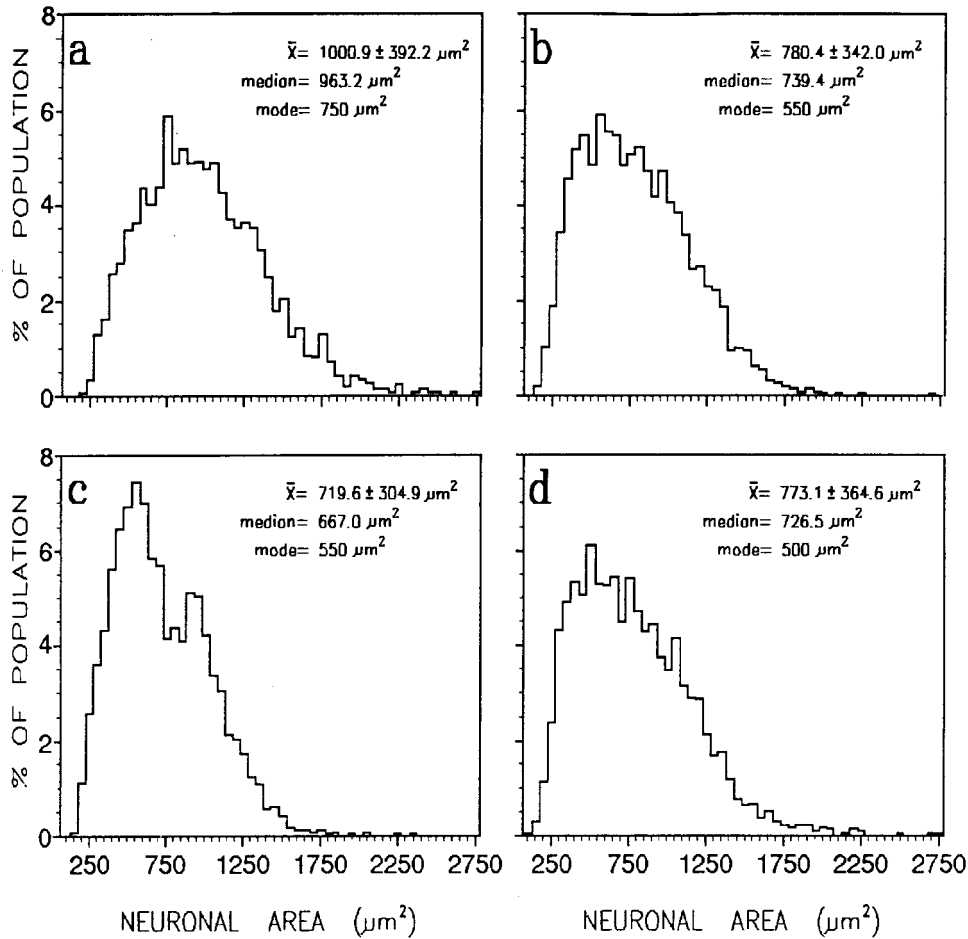


Fig 3. Neuronal somata area distributions, within petrosal ganglia from 4 different cats. a, b, c and d as in Figure 1. \bar{x} , means \pm SD.

mean neuronal somata areas were $1000.9 \pm 8.2 \mu\text{m}^2$, $780.4 \pm 5.8 \mu\text{m}^2$, $719.6 \pm 5.3 \mu\text{m}^2$ and $773.1 \pm 7.2 \mu\text{m}^2$ (mean \pm SEM) for the ganglia from male and female cats, respectively. The corresponding medians were $963.2 \mu\text{m}^2$, $739.4 \mu\text{m}^2$, $667.0 \mu\text{m}^2$ and $726.5 \mu\text{m}^2$. Distributions show that most ganglia exhibit their modes around $550 \mu\text{m}^2$ (Fig 3b-d), but the ganglion with the higher mean area had its mode displaced to $750 \mu\text{m}^2$ (Fig 3a). Nevertheless, the four frequency distributions were significantly different among them ($p < 0.01$; Kolmogorov-Smirnoff test). The ganglion with the largest mean area (Fig 3a) showed statistically significant differences with the other three ganglia in about 50% of the $50 \mu\text{m}^2$ area bins in the $150\text{-}3150 \mu\text{m}^2$ range, with maximal differences of about 28% in related bins. Conversely, although statistically significant

($p < 0.05$; Kolmogorov-Smirnoff test) differences were restricted to only 2 to 31% of the area bins between the other three ganglia, the discrepancies did not surpass 8.2% in related bins. Moreover, the two ganglia that presented no neuronal area differences diverged only in one area bin ($p < 0.05$).

DISCUSSION

The neurons of the petrosal ganglion appear to be evenly distributed within any longitudinal sectional plane, although islets of neurons separated from the surroundings by bundles of fibers were sometimes apparent in individual slices. A similar distribution has been described at the electron microscopic level in cross sections of the petrosal ganglion, indicating the presence of white

and gray matter (Stensaas and Fidone, 1977). In our preparation, such intraganglionic division between gray and white matter was not apparent, except for the fact that nerve fibers were almost absent in the perimeter of the ganglia. However, in our study neuron-containing slices comprise only part (50-70%) of the total ganglion width, leaving out the fiber containing portion of the ganglion. Thus, although the differentiation between white and gray matter can be demonstrated in transversal sections at the electron microscopic level, petrosal neurons and their fibers appear to be less segregated within longitudinal histological sections studied by means of light microscopy.

The number of neuronal somata varied between 2311 and 3429 within the four petrosal ganglia here studied. These values may be compared to previous individual observations reporting 2724 perikarya (Foley and Sackett, 1950) and 2296 perikarya (Eyzaguirre and Zapata, 1984) within the cat's petrosal ganglia. It must be noted that the somata of the superior (Ehrenritter's) ganglion were not included in this study, since we only examined 2 mm of the glossopharyngeal nerve trunk central to the petrosal ganglion, and both ganglia are 3-4 mm apart in the cat (Berger, 1980).

Although the numbers of somata within petrosal ganglia cannot be compared directly with those of other sensory ganglia, the variation observed in our study is comparable to that observed when studying thoracic (Hulsebosch *et al*, 1986; Ygge *et al*, 1981), lumbar (Schmalbruch, 1987), and sacral (Hulsebosch *et al*, 1986) dorsal root ganglia of rats. Thus, the petrosal ganglion neuronal population appears to be restrained to a relatively narrow range, with deviations that can be ascribed to individual variability, as in somatic sensory ganglia.

The neuronal somata within each petrosal ganglion seemed to have no preferential distribution along the width of the ganglion, with equal number of cells in each half of the ganglion. Most ganglia showed an almost complete axial symmetry, evidencing only small differences towards the periphery. Because no preferential plane of section was used, we cannot correlate the asymmetry found in the ganglion of one male cat with

any particular external reference point of the ganglion anatomy. Longitudinal distributions of neuronal somata constructed from cross sections indicate asymmetries in the petrosal ganglia along their cephalo-caudal axes (Stensaas and Fidone, 1977). However, these distributions were constructed from individual sections located 400 μm apart, constituting only a small sample of the total population. We can not rule out this type of organization, because the cephalo-caudal organization of the ganglia was not analyzed in our preparation.

The neuronal somata areas of most petrosal ganglia showed significant differences between them, although two of them did not reach the statistical significant level. A similar variation range could be obtained from subsets of intracellularly labeled petrosal neurons (Claps and Torrealba, 1988; Claps *et al*, 1989; Torrealba and Claps, 1988; Torrealba, 1992). Despite this individual variation, most ganglion perikaryal areas in our study were consistently confined to the 250-2250 μm^2 range, with medians and mean areas about 710 μm^2 and 758 μm^2 , respectively. These values agree with those previously reported for petrosal ganglion neurons projecting to the carotid sinus and carotid body (Claps and Torrealba, 1988; Claps *et al*, 1989; Torrealba and Claps, 1988; Torrealba, 1992).

All neuronal somata area distributions presented their modes below their respective medians and means. Indeed, modes never surpassed 7.5% of the total population. These negatively skewed distributions indicate the presence of a larger number of small cells than that expected from a normal distribution. This skewed distribution could be reflected in a large number of unmyelinated axons in the nerve, arising from the smaller neurons (Harper and Lawson, 1985; Lee *et al*, 1986). Although the glossopharyngeal nerve contains a majority of myelinated fibers (Foley and Sackett, 1950), its carotid (sinus) branch is dominated by unmyelinated fibers (Eyzaguirre and Uchizono, 1961; Fidone and Sato, 1969; McDonald, 1983). Thus, this subset of small perikarya -departing from the normal distribution of the rest- may originate the unmyelinated sensory fibers directed to the carotid body and sinus.

ACKNOWLEDGEMENTS

We want to thank Dr Fernando Torrealba for facilitating the use of the digital measuring system used to determine the neuronal areas. This work was supported by grant 1133/92 from *Fondo Nacional de Desarrollo Científico y Tecnológico* (FONDECYT).

REFERENCES

- ALCAYAGA J (1995) Arterial chemoreceptors in tissue culture: morphologic and physiologic aspects. In: GONZALEZ C, CHARRIER R, LLANOS A, RAGGI RA (eds) Second International Symposium on Altiplanic Studies. Santiago: Universidad de Chile. pp 178-182
- ALCAYAGA J, EYZAGUIRRE C (1990) Electrophysiological evidence for the reconstitution of chemosensory units in co-cultures of carotid body and nodose ganglion neurons. *Brain Res* 534: 324-328
- BELMONTE C, GALLEGO R (1983) Membrane properties of cat sensory neurones with chemoreceptor and baroreceptor endings. *J Physiol, London* 342: 603-614
- BERGER AJ (1980) The distribution of the cat's carotid sinus nerve afferent and efferent cell bodies using the horseradish peroxidase technique. *Brain Res* 190: 309-320
- CLAPS A, TORREALBA F (1988) The carotid body connection: a WGA-HRP study in the cat. *Brain Res* 455: 123-133
- CLAPS A, TORREALBA F, CALDERON F (1989) Segregation of coarse and fine glossopharyngeal axons in the visceral nucleus of the tractus solitarius of the cat. *Brain Res* 489: 80-92
- DE GROAT WC, NADELHAFT I, MORGAN C, SCHAUBLE T (1979) The central origin of efferent pathways in the carotid sinus nerve of the cat. *Science* 205: 1017-1018
- EYZAGUIRRE C, UCHIZONO K (1961) Observations on the fibre content of nerves reaching the carotid body of the cat. *J Physiol, London* 159: 268-281
- EYZAGUIRRE C, ZAPATA P (1984) Perspectives in carotid body research. *J Appl Physiol* 57: 931-957
- EYZAGUIRRE C, FITZGERALD RS, LAHIRI S, ZAPATA P (1983) Arterial chemoreceptors. In: SHEPHERD JT, ABOUD FM (eds) *Handbook of Physiology, Section 2: The Cardiovascular System, Volume 3, Peripheral Circulation and Organ Flow*. American Physiological Society. Baltimore: Williams and Wilkins. pp 557-621
- FIDONE SJ, SATO A (1969) A study of chemoreceptor and baroreceptor A and C-fibers in the cat carotid nerve. *J Physiol, London* 205: 527-548
- FOLEY JO, SACKETT WW (1950) On the number of cells and fibers in the glossopharyngeal nerve. *Anat Rec* 106: 303
- GABE M (1968) *Techniques Histologiques*. Paris: Mason et Cie
- GALLEGO R (1983) The ionic basis of action potentials in petrosal ganglion cells of the cat. *J Physiol, London* 342: 591-602
- GOLDMAN WF, SATO M, STENSAAS LJ, EYZAGUIRRE C (1987) Acetylcholine- and dopamine-induced excitation of cultured newborn rabbit nodose ganglion neurons: effects of co-culture with carotid body fragments. In: RIBEIRO JA, PALLOT DJ (eds) *Chemoreceptors in Respiratory Control*. London: Croom Helm. pp 284-295
- HARPER AA, LAWSON SN (1985) Conduction velocity is related to morphological cell type in rat dorsal root ganglion neurones. *J Physiol, London* 259: 31-46
- HULSEBOSCH CE, COGGESHALL RE, CHUNG K (1986) Numbers of rat dorsal root axons and ganglion cells during postnatal development. *Dev Brain Res* 26: 105-113
- KALIA M, DAVIES RO (1978) A neuroanatomical search for glossopharyngeal efferents to the carotid body using the retrograde transport of horseradish peroxidase. *Brain Res* 149: 477-481
- KATZ DM, BLACK IB (1986) Expression and regulation of catecholaminergic traits in primary sensory neurons: relationship to target innervation *in vivo*. *J Neurosci* 6: 983-989
- LEE KH, CHUNG K, CHUNG JM, COGGESHALL RE (1986) Correlation of cell body size, axon size, and signal conduction velocity for individually labelled dorsal root ganglion cells in the cat. *J Comp Neurol* 243: 335-346
- MCDONALD D (1983) Morphology of the rat carotid sinus nerve. II. Number and size of axons. *J Neurocytol* 12: 373-392
- MORALES A, IVORRA I, GALLEGO R (1987) Membrane properties of glossopharyngeal sensory neurons in the petrosal ganglion of the cat. *Brain Res* 401: 340-346
- NOMURA S, MIZUNO N (1982) Central distribution of afferent and efferent components of the glossopharyngeal nerve: an HRP study in the cat. *Brain Res* 236: 1-13
- SCHMALBRUCH H (1987) The number of neurons in dorsal root ganglia L4-L6 of the rat. *Anat Rec* 219: 315-322
- STENSAAS LJ, FIDONE SJ (1977) An ultrastructural study of cat petrosal ganglia: a search for autonomic ganglion cells. *Brain Res* 124: 29-39
- THEODORSSON-NORHEIM E (1986) Kruskal-Wallis test: BASIC computer program to perform nonparametric one-way analysis of variance and multiple comparisons on ranks of several independent samples. *Comput Meth Programs Biomed* 23: 57-62
- TORREALBA F (1992) Calcitonin gene-related peptide immunoreactivity in the nucleus of the tractus solitarius and the carotid receptors of the cat originates from peripheral afferents. *Neuroscience* 47: 165-173
- TORREALBA F, CLAPS C (1988) The carotid sinus connection: a WGA-HRP study in the cat. *Brain Res* 455: 134-143
- YGGE J, ALDSKOGIUS H, GRANT G (1981) Asymmetries and symmetries in the number of thoracic dorsal root ganglion cells. *J Comp Neurol* 202: 365-372

